TURBULENT CHARACTERISTICS OF A SHALLOW CONVECTIVE INTERNAL BOUNDARY LAYER

ANN-SOFI SMEDMAN and ULF HÖGSTRÖM

Department of Meteorology, University of Uppsala, Box 516, S-751 20 Uppsala, Sweden

Received in final form 16 December, 1982)

Abstract. Turbulent characteristics of a 50 to 100 m deep convective internal boundary layer (I.B.L.) have been studied. The data were gathered at a flat coastal site (Näsudden on the island of Gotland, Sweden) during three consecutive days in May 1980 which were characterized by a steady, very stable stratified marine approach flow. The site is situated on a flat area ca. 1500 m from the shoreline. Only daytime runs have been analysed in the present paper. The sensible heat flux at the ground was typically 200 W m^{-2} and was found to decrease more or less linearly with height throughout the I.B.L., being slightly negative at greater heights. The momentum flux was also found to decrease with height, but nevertheless shear production of turbulent kinetic energy was found to be large throughout the entire I.B.L.

The analysis shows that the turbulent regime has a mixed character. Certain characteristics, such as the rate of growth of the I.B.L., appear to be almost entirely controlled by mechanical turbulence, while others, notably temperature variance and the spectrum of vertical velocity, scale remarkably well with w_* and z_i, in accordance with the results found in fully convective conditions during the experiments at Minnesota and Aschurch. Other turbulent characteristics, such as spectra of the horizontal wind components measured near the top of the I.B.L. tend to adhere to mixed-layer scaling in the high frequency range, exhibiting much increased energy in the lower (reduced) frequency range.

Spectra of the velocity components from 10 m are shown to be in general agreement with findings from 'ideal', homogeneous sites (Kansas) when properly normalized, although the low frequency part of u- and v-spectra are slightly reduced compared to the case with deep convection.

1. Introduction

The study presented in this paper is based on measurements from three days in May 1980 at the Näsudden wind power test site (a 2.5 MW machine began operating in late 1982) on the island of Gotland in the Baltic. The site is situated on a flat peninsula, covered mainly with scattered juniper bushes. During the measurement period analysed here, May 28 to May 30, 1980, there was a steady flow from a sector between east and southeast. As seen from Figure 1, this means that the flow, coming from the Baltic, has to pass a ca. 5 km wide strip of land – a fairly flat, mainly agricultural area – and then again encounters a ca. 3 km wide stretch of open water, before it enters the Näsudden peninsula, where the measurement site is situated 1200–1800 m farther inland.

In this paper only daytime data are analysed. The data set thus selected comprises continuous wind and temperature profiles up to 145 m on a tower and eight hours of turbulence measurements, from the levels 10, 75, and 135 m, although not all the time at three levels simultaneously, cf. next section. In addition, radiosonde data from the site are used as a general background.

The turbulence data were obtained using a fast response windvane-based hotwire system, which measures the instantaneous values of temperature, wind direction and the three components of the wind (Högström *et al.*, 1980). Data were sampled at 20 Hz

Boundary-Layer Meteorology **25** (1983) 271–287. 0006–8314/83/0253–0271$02.55.

Fig. 1. The island of Gotland showing the measuring site Näsudden.

on magnetic tape in one-hour periods and processed on a IBM 360/370 computer. Before moments and spectra were evaluated, the data were corrected for an aerodynamic error, according to the findings in Högström (1982). A 1024-point Fast Fourier Transform routine (*S*tatistical *A*nalysis *S*ystem) was used to compute spectra in two separate, slightly overlapping bands.

2. Observed Characteristics

The general meteorological situation in the area of the Baltic Sea was quite steady during the period of our measurements, which lasted from 10 h on May 28 to about 14 h on

May 30, 1980. The 1000 mb geostrophic wind was from a southeasterly direction, 10–14 m s^{-1} most of the time, decreasing, however, to 5 m s^{-1} on May 30. The temperature of the sea surface was quite low, ca. 5 °C over most of the area between the mainland of the Baltic states and Gotland. As the air mass was appreciably warmer – midday temperatures in Estonia were typically 20–22 °C – a strong inversion characterized the lower parts of the atmosphere over the sea. According to the temperature soundings, the top of this inversion was at ca. 200 m above the sea surface, with a corresponding temperature maximum of 17 °C. This very strong inversion was also present in the daytime temperature profiles from the Näsudden 145 m tower, as is seen from the typical profiles shown in Figure 2a and b. These figures also show the unstable internal boundary layer formed in the lowest layer over the heated land of the Näsudden peninsula. A detailed study of the turbulent characteristics of this layer is the main theme of this paper. But before we embark on that task, we want to get an idea of the turbulence structure in the inversion layer above.

Four daytime runs were performed at 135 m. The gradient Richardson number, Ri, for three of them was far above the critical value, 0.25, while Ri = 0.22 for the remaining case.

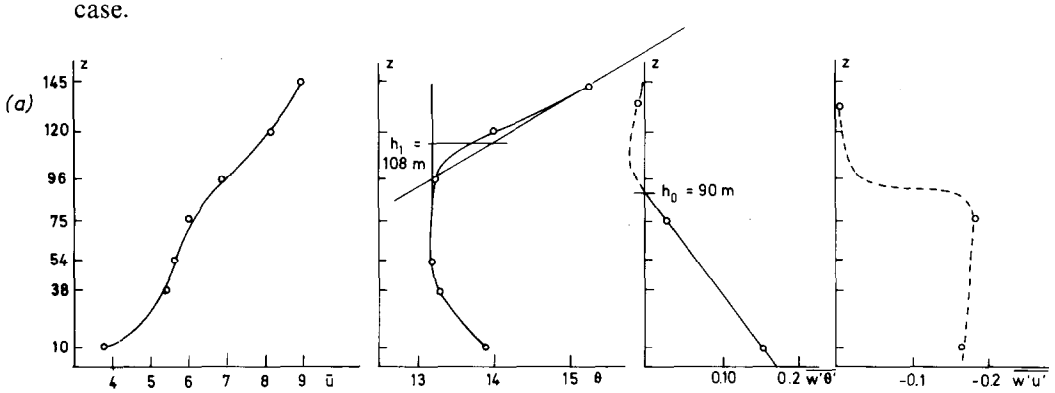

Fig. 2a. Various profiles from Näsudden, run N1 (cf. Table I). The profiles are, from left to right: wind-speed, potential temperature, temperature flux and momentum flux. The two mixing-height concepts used in the paper are illustrated, h_0 being the 'z_i' of Table I and h_1 'the slab model height' (cf. Figure 5 and the text).

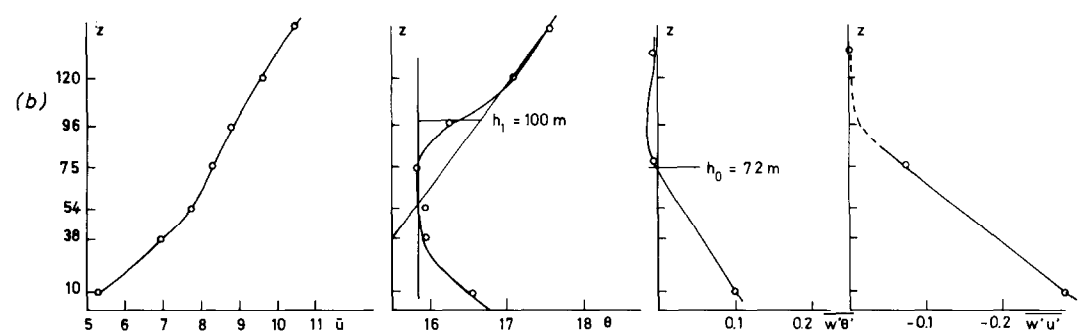

Fig. 2b. Same as Figure 2a but run N2 (cf. Table I).

Figure 3 shows spectra of the vertical velocity component for one of the runs with $Ri > Ri_{crit.}$ (N2; cf. Table I) and for the run with Ri = 0.22 (N11). It is clear that the flow at 135 m is not fully turbulent in run N2 in contrast with the flow in run N11. Generally speaking, the flow at 135 m is not fully turbulent, and the spectra are close to the noise level in the high frequency end, but bursts of turbulence occur; at lower frequencies, waves and other mesoscale motions are present – phenomena which will be the subject of a forthcoming study.

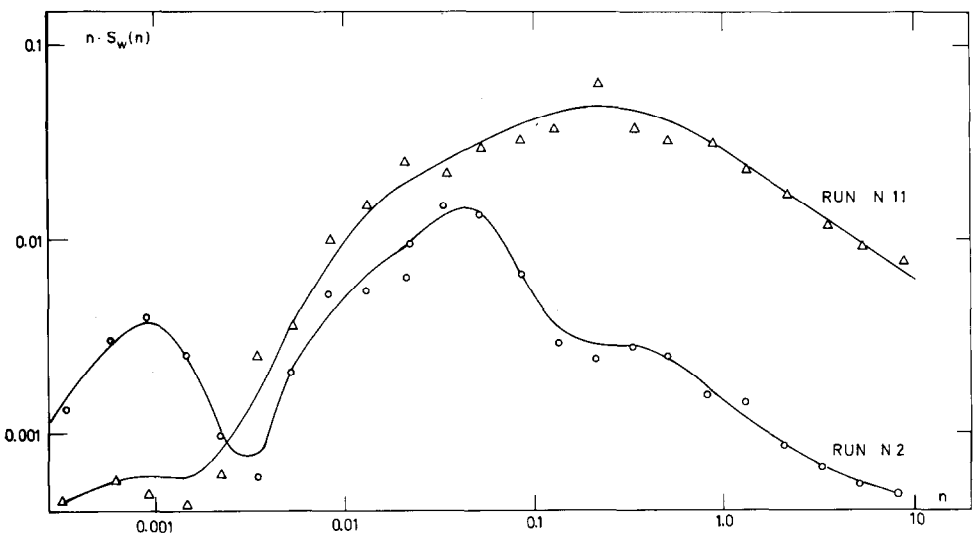

Fig. 3. Examples of spectra of the vertical wind component from 135 m. Symbols: ○ = run N2, with Ri = 0.6; △ = run N11, with Ri = 0.22.

Table I is a summary of some relevant data for the turbulence runs. Figure 2a and b show examples of profiles of wind-speed, potential temperature, temperature flux and momentum flux. As seen from these plots, the temperature flux (or heat flux) decreases more or less linearly up to a certain level where the flux changes sign, attains a negative maximum, the magnitude of which is of the order 20% of the surface heat flux, and then gradually approaches zero with height. In Table I the mixing height z_i has been defined as the height where the heat flux is zero. The momentum flux also decreases with height – in all cases except runs N0 and N1 (Figure 2a) – rather rapidly.

3. Framework of Analysis

Figure 4 is from Nicholls and Readings (1979) showing idealized limits of validity of various scaling techniques used in atmospheric boundary layer studies. As discussed by these authors, Monin-Obukhov surface-layer theory, including the special case of free convection, is expected to be valid below the horizontal line $z/z_i = 0.1$, while mixed-layer scaling is likely to be valid in the rhombic area in the upper right-hand corner, denoted

TABLE I

Summary of data from the turbulence runs. Duration of runs: 60 min, except for run N0 which was only 30 min long. z_i is obtained from plotted heat-flux profiles as the level where the flux = 0.

Run No.	Date	Time (local)	u_*	$-L$	z_i	w_*	θ_* $\overline{w'\theta'}/w_*$	10 m			75 m			135 m		
								$\overline{U}$	$-\overline{u'w'}$	$\overline{w'\theta'}$	$\overline{U}$	$-\overline{u'w'}$	$\overline{w'\theta'}$	$\overline{U}$	$-\overline{u'w'}$	$\overline{w'\theta'}$
N0[a]	28/5	12.03	0.35	22	87	0.77	0.197	4.1	0.124	0.145	5.5	0.122	0.105			
N1	28/5	14.47	0.41	28	90	0.82	0.214	3.7	0.166	0.156	6.0	0.186	0.031	9.0	0.005	−0.007
N2	28/5	16.13	0.53	98	72	0.65	0.169	5.3	0.282	0.098	8.2	0.081	−0.006	10.4	0.009	−0.009
N3	28/5	17.35	0.55	168	70	0.55	0.127	5.1	0.303	0.056	10.4	0.091	−0.06	13.0	0.025	−0.021
N11	29/5	10.52	0.60	136	50	0.58	0.209	6.7	0.355	0.100				14.0	0.025	−0.009
N12	29/5	15.31	0.37	25	86	0.76	0.192	3.1	0.140	0.124	5.8	0.120	0.015			
N13	30/5	10.10	0.42	94	67	0.51	0.101	4.2	0.174	0.046	7.0	0.060	−0.013			
N14	30/5	12.00	0.29	35	86	0.55	0.092	3.1	0.085	0.052	4.3	0.055	0.017			
N15[b]	30/5	13.00	0.36	35	80	0.64	0.197	3.7	0.131	0.082	3.6	0.006	0.006			

[a] This run is only 30 min long; no spectra were evaluated.

[b] No spectra were evaluated for this run (for technical reasons).

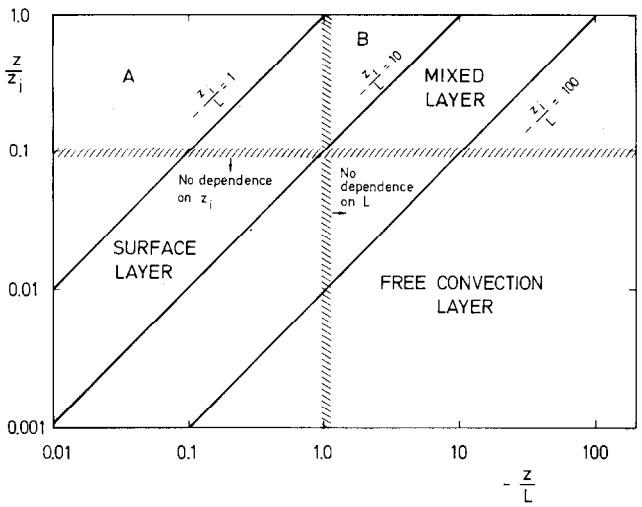

Fig. 4. Schematic diagram showing idealized limits of validity of certain scaling techniques (see text for description). After Nicholls and Readings (1979).

by 'Mixed layer'. Nicholls and Readings present results from measurements representing the area 'A' of the diagram and show that it is necessary to introduce a scaling technique that takes into account both thermal convection and mechanical mixing in order to describe the turbulent characteristics of the particular flow regime that they were studying (the unstable marine boundary layer). From Table I we conclude that our 10 m data fall in the (upper part of) the lower left corner, whereas some of the 75 m runs fall in the area denoted by 'B' (those having z/z_i-values less than 1.0). The remaining 75 m runs as well as the 135 m runs represent conditions outside the boundary layer ($z > z_i$), which are not included in the diagram.

The above general considerations will serve as a background to the analysis of the turbulence characteristics within the convective internal boundary layer to be presented in the next few sections.

4. The Height of the Convective Layer

As a first task, we shall try to determine the mechanism mainly responsible for the growth of the unstable internal boundary layer. In our attempt to do so, we shall take account of the fact that turbulence was intermittent in the upper stable part of the 150 m deep profile observed on the mast. It is reasonable then to make the following assumptions concerning the approach flow:

(1) There is a strong, ground-based inversion in the lowest 200 m of the atmosphere at the point where the air first encounters the Näsudden peninsula. Such a temperature profile is indeed likely in view of the profiles observed at the mast 1300–1800 m inland – see Figure 2a and b – knowing that the surface temperature of the bay east of the peninsula was ca. 8 °C.

(2) The level of turbulence of the approach flow is very low. This is confirmed by the measurements at 135 m referred to in Section 2.

Thus it is reasonable to assume that the turbulence observed in the lowest 50–100 m at the mast is almost exclusively generated by the combined action of thermal convection and shearing stress set up at the land-air interface during the passage of the air from the shoreline to the mast. We now propose to study this modification process by analogy with the continuous build-up of a convective boundary layer over an horizontally homogeneous area. This implies that in the rate equation, i.e., in the equation for $\mathrm{d}h/\mathrm{d}t$, x/U is substituted for time, where x is travel distance from the shoreline and U is the corresponding wind speed. Analysing an extensive set of field data, Driedonks (1981) showed that the rate of growth of the horizontally homogeneous convective daytime boundary layer is well described by the following formula by Tennekes:

$$\frac{\mathrm{d}h}{\mathrm{d}t} = C_F \sigma_w^3 / h \Delta b \tag{1}$$

with

$$\sigma_w^3 = w_*^3 + (A/C_F) u_*^3 \tag{2}$$

and

$$\Delta b = (g/T_0) \Delta\theta \tag{3}$$

$$w_*^3 = (g/T_0) \cdot \overline{\theta' w'} \cdot h \,. \tag{4}$$

Here h is the 'height of the boundary layer' (definition, see below) at time t and $\Delta\theta$ is the temperature jump at the top of that layer, according to the concept of the idealized 'slab model' (see below), and C_F and A are constants. With $C_F = 0.2$ and $A = 5$, Driedonks found that Equation (1), after integration, describes observed h-values over the entire range of observations from almost zero to over 1000 m without significant bias.

Equations (1) and (2) stem from a parameterization of the equation of turbulent energy in the entrainment zone, cf., Tennekes and Driedonks (1981). The inclusion of the two terms w_*^3 and $(A/C_F)u_*^3$ in (2) means that convective mixing (through w_*^3) as well as mechanical mixing are taken into account. As shown by Driedonks (1981), the mechanical term strongly dominates the early morning stage of development, whereas the convective term alone gives a good estimate of the midday height.

'The slab model' referred to above implies a constant potential temperature layer up to a height h, where there is a positive jump $\Delta\theta$ in the potential temperature; above h, θ increases at a constant rate $\partial\theta/\partial z = \gamma_0$, see Figure 5. That figure also shows how h and $\Delta\theta$ are obtained from a real θ-profile. It should be observed that the boundary-layer height defined in this way differs from the definition adopted in Table I for z_i.

We shall now apply Tennekes' model, Equations (1)–(4), to our present data from Näsudden. Equations (1)–(4) can be combined to give:

$$\frac{\mathrm{d}h}{\mathrm{d}t} = C_F \frac{\overline{\theta' w'}}{\Delta\theta} + A \frac{u_*^3 T_0}{g \Delta\theta} \cdot \frac{1}{h} \,. \tag{6}$$

This differential equation can be integrated numerically, if we are able to specify the parameters $\overline{\theta' w'}$, $\Delta\theta$, and u_* as functions of time. In our case, we have access to data for these parameters only at the tower, so we take the observed values as constants over the integration regime, i.e.,

$$\frac{dh}{dt} = \alpha + \beta \frac{1}{h} \tag{6b}$$

with α and β constant for the individual runs. The temperature jump $\Delta\theta$ is obtained from the profiles in the way schematically illustrated in Figure 5. Figure 2a and b illustrate the procedure for two of the runs (h_1 of Figure 2a and b).

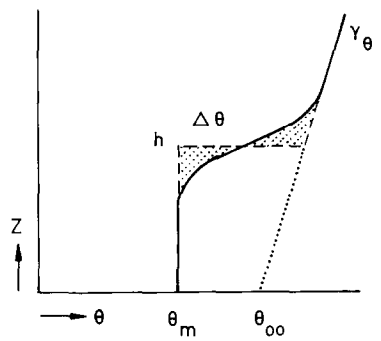

Fig. 5. Measured profile of θ (—) and 'the slab model assumption (––)', giving the mixing depth h. After Driedonks (1981).

The integration of Equation (6b) should start from $h = h_0 \neq 0$ at $t = 0$ as shown by Driedonks (1981). But this requires detailed information about the initial temperature profile which we do not have, so we simply assume $h_0 = 0$.

In order to get an idea of the relative importance of the various possible mechanisms in creating the observing unstable I.B.L., three simplified approaches for determining h were applied in addition to the solution of Equation (6b). They are:

(1) 'Encroachment', i.e., no entrainment is assumed to occur. The resulting equation is (cf., Driedonks, 1981):

$$h = \sqrt{\frac{2(\overline{\theta' w'})_0}{\gamma_\theta} \cdot t} = h_e .$$

(2) Tennekes' formula with the u_*-term equal to zero, which implies boundary-layer growth simply due to convection. This assumption is equivalent to $\beta = 0$ in Equation (6b), so that

$$h = \alpha \cdot t = h_c .$$

(3) Tennekes' formula with the thermal convection term equal to zero, i.e., $\alpha = 0$. From Equation (6b) we get

$$h = \sqrt{2\beta t} = h_* .$$

The result of the calculation (based on 8 out of the 9 cases listed in Table I†) is

$\bar{h}_{obs}$	$\bar{h}_e$	$\bar{h}_c$	$\bar{h}_*$	$\bar{h}_T$
103	41	9	95	99

where $\bar{h}_{obs}$ is the mean of the observed heights, h_T the mean height calculated with the full Equation (6b) and the remaining symbols are as listed above. Apparently Tennekes' Equation gives a good estimate of the height: the bias $\bar{h}_{obs} - \bar{h}_T$ being 4 m and the corresponding standard deviation 26 m. The fact that $\bar{h}_*$ has nearly the same value as $\bar{h}_T$ but $\bar{h}_c$ is a factor 10 lower shows the dominating influence of mechanical turbulence on the growth of the I.B.L. This is not at all a trivial result, as the heat flux at the ground is fairly large, 150–200 W m^{-2}. We also observe that $\bar{h}_e$ is low by a factor 2.5 compared with the observed mean height. This clearly indicates that entrainment is important for the formation of the I.B.L.

Although the simplifications introduced in the analysis – fluxes and $\Delta\theta$ independent of travel time, $h_0 = 0$ – prohibit a truly quantitative test of the various formulae, the general conclusions, as stated above, are likely to be valid.

5. Variances of the Wind Components and of Temperature

The standard deviation of the vertical component normalized with u_* is known to be a function of z/L in the homogeneous surface layer. Figure 6 shows that this holds true

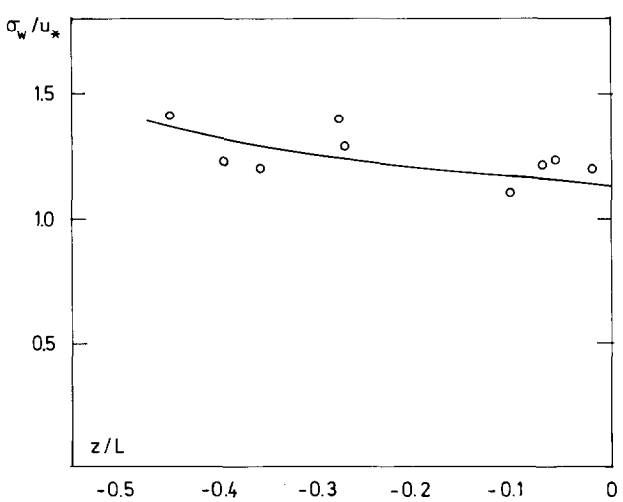

Fig. 6. Measured values of the normalized standard deviation of the vertical velocity, σ_w/u_*, at 10 m as a function of z/L.

† In one of the runs, N15, the slab model could not be applied.

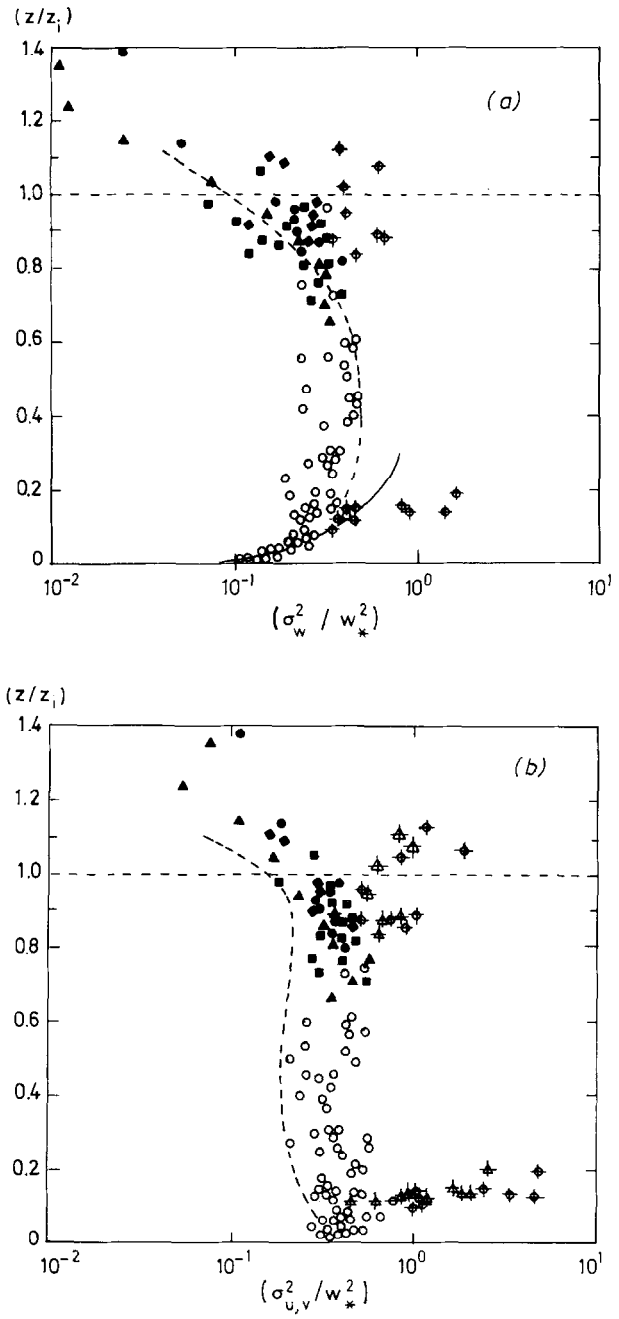

Fig. 7. (a) Normalized vertical velocity variance σ_w^2/w_*^2. The solid line is the free convection prediction. Symbols: ⊕ are data from Näsudden (10 and 75 m) and the remaining data points are from Minnesota and Aschurch. (b) Horizontal velocity variances normalized by w_*^2. Symbols ⊕: σ_u^2/w_*^2 from Näsudden and ⧋: σ_v^2/w_*^2 from Näsudden. Other symbols are the average of the horizontal components $\sigma_{u,v}^2$ from Minnesota and from Aschurch. Dashed lines represent the average of the S1 and S2 cases in Willis and Deardorff (1974). Adapted after Caughey and Palmer (1979).

for the Näsudden 10 m data also, the trend being similar to that found in Kansas (Haugen *et al.*, 1970) and the scatter being small. In Figure 7a, the 10 m data as well as the 75 m data for σ_w^2 have been normalized with w_*^2 and plotted against z/z_i together with the data obtained in the Minnesota and the Aschurch experiments (from Caughey and Palmer, 1979). The solid line is the free convection prediction. Five of the nine data points from 10 m fall very close to this line, while the remaining four are far out, being larger by a factor of 2 or 3. Inspection of the data reveals the reason for this behaviour. The five points on the line have $-z/L$-values above ca. 0.3 while the other four have values below or close to 0.1. The latter group of data thus represent forced convection conditions.

The 75 m data are generally larger than the data from Minnesota and Aschurch for corresponding z/z_i–values. The difference is relatively small near $z/z_i = 0.8$, but increases with dimensionless height. This increase is probably due to mechanical mixing, which was shown in the last section to be an active mechanism for the growth of the I.B.L. and hence for entrainment. This explanation is further substantiated by the magnitude of the shear production term of the turbulent kinetic energy budget at 75 m. If normalized with mixed-layer scales, this term equals:

$$\left(\overline{u'w'}\,\frac{\partial \bar{u}}{\partial z} + \overline{v'w'}\,\frac{\partial \bar{v}}{\partial z}\right)(z_i/w_*^3)\,.$$

A typical value of this quantity for the Näsudden 75 m data is 0.5. According to Caughey and Wyngaard (1979), this term is about 0.1 at $z/z_i = 0.1$ in the well mixed boundary layer and decreases rapidly to very insignificant values. It is interesting to note that the buoyancy production term

$$\{-(g/T)\overline{w'\theta'}\}\,(z_i/w_*^3)$$

is about 1.0 at 10 m at Näsudden ($z/z_i \approx 0.1$), which is in general agreement with the findings reported in Caughey and Wyngaard, as is also the general linear decrease of this term up to the top of the I.B.L.

For the horizontal wind components, normalization of the standard deviations at 10 m with u_* gives the following results:

$$\sigma_u/u_* = 2.04 \pm 0.15$$

$$\sigma_v/u_* = 1.71 \pm 0.25\,.$$

According to Panofsky *et al.* (1977), these quantities have been found to scale with z_i/L:

$$\sigma_u/u_* = \sigma_v/u_* = (12 - 0.5\,z_i/L)^{1/3}\,.$$

In our case, this yields values in a very narrow range: 2.29 – 2.39, and it was not possible to distinguish such a trend. It is also noted that the observed σ_u/u_*-values are ca. 10% lower than expected and the σ_v/u_*-values ca. 25% lower. We will return to this anomaly when discussing the corresponding spectra in the next section.

In Figure 7b the variance data for the horizontal components have been expressed

in mixed-layer scaling terms and can therefore be compared with measurements from Minnesota and Aschurch. The 10 m-data form two groups: those with $-z/L > 0.3$ have σ^2/w_*^2-values 1–2 times larger than the average mixed-layer data; and those with $-z/L < 0.1$ have values 5–10 times larger. The 75 m data are much larger than the Aschurch data in the upper part of the entrainment zone but seem to converge to these data near $z/z_i = 0.8$, like the w-data do.

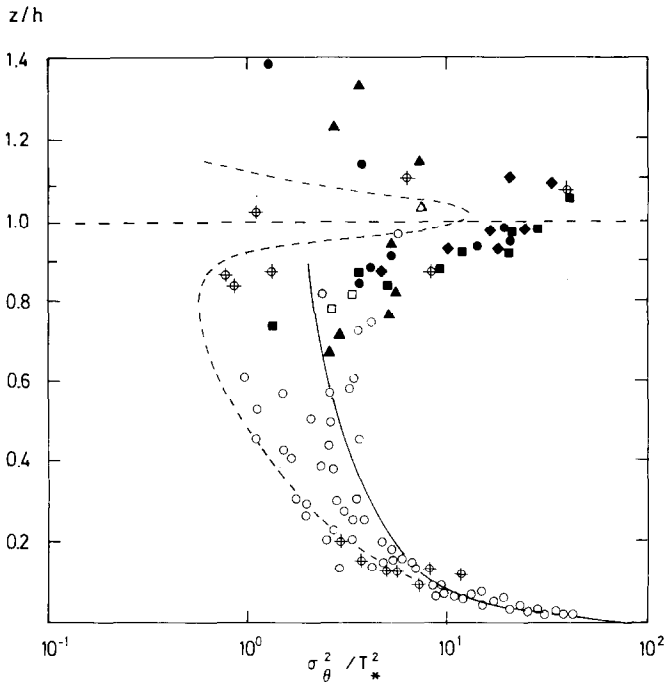

Fig. 8. The normalized temperature variance. The solid line represents the free convection prediction and the dashed line the S1 case from Willis and Deardorff (1974). Symbols ⊕ are data from Näsudden (10 and 75 m); the remaining data points are from Minnesota and Aschurch. Adapted after Caughey and Palmer (1979).

The temperature variance data from 10 and 75 m have been expressed in mixed-layer scales and plotted in Figure 8 together with corresponding data from Minnesota and Aschurch. The 10 m data come remarkably close to the dashed line which represent laboratory data of Willis and Deardorff (1974) (their S1 case). Also the three 75 m points having the lowest z/z_i-values come close to that curve, while 3 out of the 4 remaining cases agree quite well with the Aschurch data. The reason why the temperature data follow the trend of the 'ideal' mixed-layer data is not clear. In analysing the Kansas surface-layer data, Wyngaard *et al.* (1971) noted that the normalized temperature variance approached the free convection prediction limit at remarkably low $-z/L$-values, a result also found by Högström and Smedman-Högström (1974).

6. Wind Spectra

Spectra of the wind components at 10 m have been normalized by $u_*^2 \phi_\varepsilon^{2/3}$, where ϕ_ε is the nondimensional dissipation rate. This quantity has been evaluated from the expression (Kaimal *et al.*, 1972):

$$\phi_\varepsilon^{2/3} = 1 + 0.5\,|z/L|^{2/3}\,.$$

Figure 9 and 10 show w-, and u-spectral plots, respectively. The curves drawn are from the Kansas experiment (Kaimal *et al.*, 1972). In the inertial subrange region, the data points cluster without noticable bias along the respective curve, the scatter being least for the u-component. In the low frequency region, the Kansas curves for the three components behave differently with respect to separation according to z/L. Thus the w-spectra order themselves nicely in the region $0 > z/L > -0.3$, while the more unstable runs fill up a relatively limited area, cf. Figure 9. Our data lie in the interval $-0.02 > z/L > -0.45$ with a mean $z/L = -0.22$. It is not possible to distinguish a trend among our data points, but in the mean, they do come close to the Kansas curve for our mean z/L.

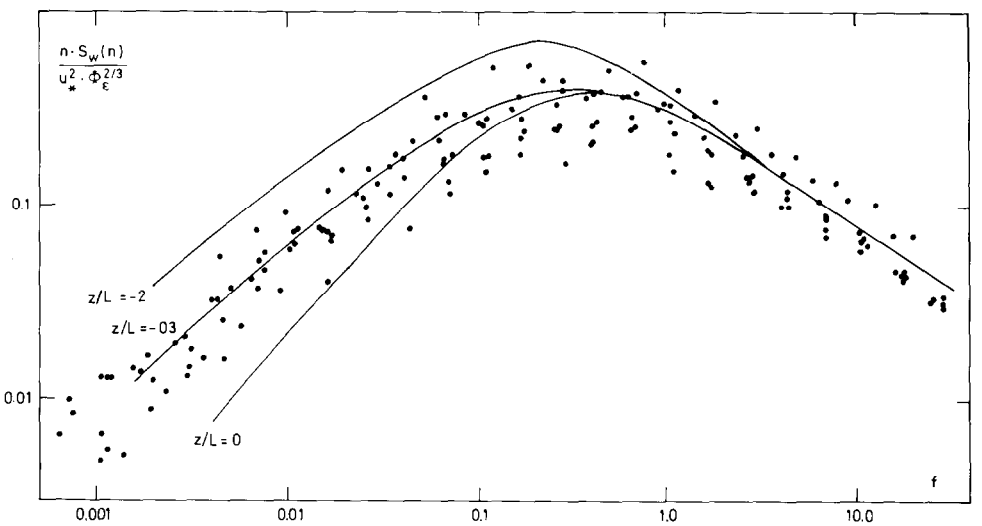

Fig. 9. Surface-layer normalized 10 m vertical velocity spectra together with the corresponding curves from Kaimal *et al.* (1972) for unstable and neutral stratification.

The low-frequency range of the Kansas u-spectra exhibit 'an excluded region', between the curve for $z/L = 0$ and a curve delineating the lower limit of the range for the unstable spectral curves. Our spectra for u (Figure 10) exhibit appreciable scatter in the low frequency range. Rather than avoiding 'the excluded region', the data points have their center of gravity in this area. Referring back to the discussion of the normalized variance σ_u/u_* of the previous section, we can now trace the relative

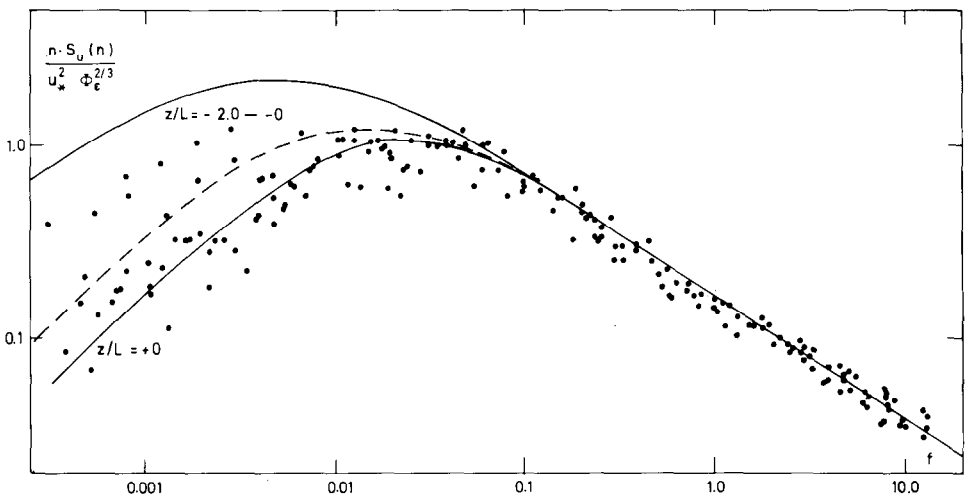

Fig. 10. Surface layer normalized 10 m longitudinal spectra together with the corresponding curves from Kaimal *et al.* (1972) for unstable and neutral stratification.

reduction in the magnitude of this quantity to the low frequency end of the spectrum. The reason for this reduction is no doubt the very limited depth of the convective layer, the energy of the horizontal components in this spectral region being largely derived from deep convection return flow (Wyngaard and Coté, 1974). The same general reasoning also applies to the v-spectra (not shown here).

In three of our runs, the 75 m level is below the inversion (actually five runs, but no spectra were evaluated for runs N0 and N15, cf. Table I), z/z_i in these cases being in the range 0.83 to 0.87. Figure 11 and 12 display the measured w-, and u-spectra respectively normalized with $w_*^2 \Psi_\varepsilon^{2/3}$ and plotted against $f_i = nz_i/\bar{u}$. The solid curves drawn are the corresponding curves observed in the Minnesota experiment (Kaimal *et al.*, 1976) for the z/z_i-range 0.2–1.0 for w and 0.02–1.0 for u. For the dimensionless dissipation parameter Ψ_ε, a value was chosen so as to get the inertial subrange data for the u-spectrum as close as possible to the Minnesota curve. This procedure gives $\Psi_\varepsilon = 0.8$. The corresponding mean value obtained in the Aschurch experiment for $z/z_i \approx 0.8$ is ca. 0.5 (Caughey and Palmer, 1979), but the data points scatter in the range 0.3 to 0.8. Kaimal *et al.* (1976) obtain values between 0.5 and 0.7 "for the fully convective runs" and "slightly larger values in the near transition runs", their Figure 4 indicating a value near 0.8 for these cases.

As seen from Figure 11, the w-spectra appear to follow the corresponding Minnesota curve reasonably well over the entire frequency range. The observed spectra values near the peak are, however, larger, but it is doubtful whether this result is significant.

The observed spectra of the longitudinal wind components, Figure 12, have appreciably more low frequency energy than the corresponding Minnesota curves (if the spectra are compared on a reduced frequency scale, as here). It is reasonable to think that this excess energy is due to mechanical turbulence, which is absent in the fully

convective layer, decreasing linearly with height in the I.B.L. In contrast to the fully convective case, however, shear production was also large, even in the upper layers of the I.B.L.

The rate of growth of the I.B.L. was shown to be controlled almost entirely by mechanical mixing, the observed height of the I.B.L. at the measuring site ca. 1.5 km from the shoreline being remarkably well predicted by a formula based on the Tennekes entrainment hypothesis.

Velocity variances and spectra at 10 m normalized with surface-layer scales were found to be in general agreement with corresponding values from Kansas and other homogeneous sites, the most notable deviations being σ_u/u_* and σ_v/u_*, which were smaller than their ideal counterparts by 10 and 25%, respectively.

The variances of the velocity components divided by w_*^2 for 10 and 75 m were compared with corresponding results from fully convective conditions in Minnesota and Aschurch. The 10 m data for σ_w^2/w_*^2 were found to fall into two distinct groups according to z/L-values: those with $-z/L > 0.3$, representing free convection, are in agreement with earlier data; the other group with $-z/L$-values < 0.1, representing forced convection, are far out. The 75 m data appear to converge to the 'fully convective' results in their lower z/z_i-range around 0.8, while those data that represent the upper part of the entrainment zone ($z/z_i \approx 1.1$) are larger than the corresponding Aschurch data by almost a factor of 10. This feature is attributed to increased entrainment by mechanical mixing.

The normalized variance data for the horizontal components show a very similar behaviour in the z/z_i-range 0.8–1.1 as does the variance of the vertical component. At the lower level, much higher normalized variances are observed compared to the fully convective case.

The normalized temperature variance $\sigma_\theta^2/\theta_*^2$, where $\theta_* = \overline{w'\theta'}/w_*$, was also compared with corresponding data from Minnesota and Aschurch and with laboratory data of Willis and Deardorff (1974). The data from Näsudden were found to be in agreement with these data over the entire range of z/z_i, 0.1–1.1.

Velocity spectra were available for three runs for the z/z_i-range 0.8–0.9. These spectra were normalized with $w_*^2 \Psi_\varepsilon^{2/3}$ and plotted against $f_i = nz_i/\bar{u}$. The normalized spectral data for u and w were found to be in agreement with 'the fully convective' results in the inertial subrange provided Ψ_ε was made equal to 0.8. This value is only slightly higher than the mean value obtained in Aschurch for this quantity at z/z_i around 0.8. In the low frequency range (in f_i), the spectral estimates for w agree with 'the fully convective' curve, while those for the u- and v-components have much higher energy than the corresponding curves in this frequency range.

Acknowledgement

The authors wish to express their sincere thanks to Hans Bergström, Hans Alexandersson, Torgny Faxén, Leif Enger and Knut Lundin of our institute and Tord Kvick of the Swedish Meteorological and Hydrological Institute who made the field experiment

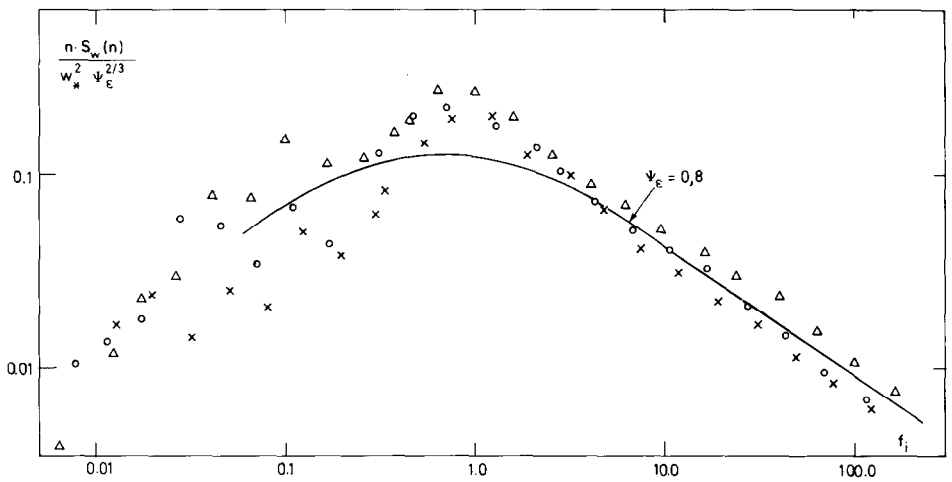

Fig. 11. Mixed-layer normalized 75 m vertical velocity spectra. The curve is from Kaimal *et al.* (1976) for $z/z_i = 0.2–1.0$ and with $\Psi_\varepsilon = 0.8$.

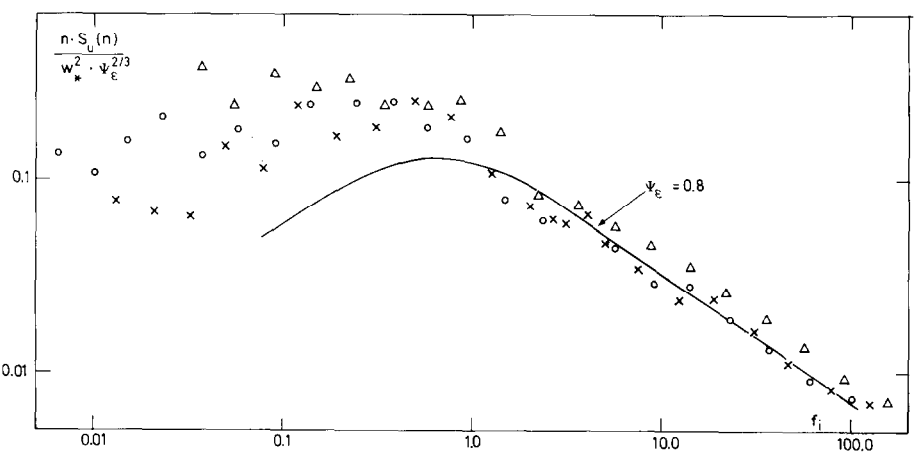

Fig. 12. Mixed-layer normalized 75 m u-spectra. The curve is from Kaimal *et al.* (1976) for $z/z_i = 0.02–1.0$, with $\Psi_\varepsilon = 0.8$.

convective cases represented by the solid curves. A very similar result was found for the v-spectra (not shown here).

7. Conclusions

The analysis has shown how the turbulent characteristics of the shallow unstable internal boundary layer studied are mechanically as well as thermally induced. Thus buoyant production of turbulent kinetic energy is shown to be as large as in the fully

possible. Thanks are also given to Miss Marianne Björklund for typing the manuscript and to Mrs Aina Ekström and Mrs Ulla Lindqvist for drawing the figures.

The field experiment was sponsored by the National Swedish Board for Energy Source Development (NE contract No 5061 472). The analysis was supported in part by the Swedish Natural Science Research Council (NFR contract No E-EG 3556-100).

References

Caughey, S. J. and Wyngaard, J. C.: 1979, 'The Turbulence Kinetic Energy Budget in Convective Conditions', *Quart. J. Roy. Meteorol. Soc.* **105**, 231–239.

Caughey, S. J. and Palmer, S. G.: 1979, 'Some Aspects of Turbulence Structure Through the Depth of the Convective Boundary Layer', *Quart. J. Roy. Meteorol. Soc.* **105**, 811–827.

Driedonks, A. G. M.: 1981, 'Dynamics of the Well-Mixed Atmospheric Boundary Layer'. KNMI Scientific Report W.R. 81–2, pp. 189, De Bilt.

Haugen, D. A., Kaimal, J. C., and Bradley, E. F.: 1971, 'An Experimental Study of Reynolds Stress and Heat Flux in the Atmospheric Surface Layer', *Quart. J. Roy. Meteorol. Soc.* **97**, 168–180.

Högström, U. and Smedman-Högström, A.-S.: 1974, 'Turbulence Mechanisms at an Agricultural Site', *Boundary-Layer Meteorol.* **7**, 373–389.

Högström, U., Enger, L., and Knudsen, E.: 1980, 'A Complete System for Probing the Detailed Structure of Atmospheric Boundary Layer Flow', Meteorol. Inst. Uppsala, Report No. 60, Uppsala, Sweden.

Högström, U.: 1982, 'A Critical Evaluation of the Aerodynamical Error of a Turbulence Instrument', Accepted for publ. in *J. Appl. Meteorol.*

Kaimal, J. C., Wyngaard, J. C., Izumi, Y., and Coté, O. R.: 1972, 'Spectral Characteristics of Surface Layer Turbulence', *Quart. J. Roy. Meteorol. Soc.* **98**, 563–589.

Kaimal, J. C., Wyngaard, J. C., Haugen, D. A., Coté, O. R., Izumi, Y., Caughey, S. J., and Readings, C. Y.: 1976, 'Turbulence Structure in the Convective Boundary Layer', *J. Atmospheric Sci.* **33**, 2152–2169.

Nicholls, S. and Readings, C. J.: 1979, 'Aircraft Observations of the Structure of the Lower Boundary Layer Over the Sea', *Quart. J. Roy. Meteorol. Soc.* **105**, 785–802.

Panofsky, H. A., Tennekes, H., Lenschow, D. H., and Wyngaard, J. C.: 1977, 'The Characteristics of Turbulent Velocity Components in the Surface Layer Under Convective Conditions', *Boundary-Layer Meteorol.* **11**, 355–361.

Tennekes, H. and Driedonks, A. G. M.: 1981, 'Basic Entrainment Equations For the Atmospheric Boundary Layer', *Boundary-Layer Meteorol.* **20**, 515–531.

Willis, G. E. and Deardorff, J. W.: 1974, 'A Laboratory Model of the Unstable Planetary Boundary Layer', *J. Atmospheric Sci.* **31**, 1297–1307.

Wyngaard, J. C., Coté, O. R., and Izumi, Y.: 1971, 'Local Free Convection, Similarity and the Budgets of Shear Stress and Heat Flux', *J. Atmospheric Sci.* **28**, 1171–1182.

Wyngaard, J. C. and Coté, O. R.: 1974, 'The Evolution of a Convective Planetary Boundary Layer – a Higher-Order-Closure Model Study', *Boundary-Layer Meteorol.* **7**, 289–308.